HEPCAT Year 1 Report: Progress of the CHILLAX Experiment

James Kingston

2024-03-31

Document Description

In this report I will discuss the work I have done since I have begun my HEPCAT fellowship, which is the period of January 2023 - March 2024. I will also discuss my research plans for the remainder of the fellowship as well as of my PhD.

Introduction

A significant facet of modern experimental particle physics research is that of searching for hypothetical rare events. In this context, "rare" means "unusual to detect in the laboratory", and can be a confirmed phenomenon (e.g. coherent elastic neutrino-nucleus scattering, which has a high cross section at low, difficult to detect energies), or an as-of-yet unobserved phenomenon that may not exist (e.g. dark matter - standard model matter non-gravitational interaction). A salient challenge for experimentalists is to devise detectors optimized for observing such rare events.

Noble elements are widely used target media for low-cross section experiments. Noble liquids are brilliant scintillators, scalable, capable of ultrahigh chemical purity and radiopurity, and produce independently detectable scintillation and ionization. Ionized electrons in pure noble elements have long lifetimes (O(1 ms)), a property that allows for low electron attenuation. The two primary noble liquids used in rare event searches are argon and xenon. Argon and xenon each have relative advantageous properties relative to each other that make one more approriate than the other for certain applicatons. Argon is a good kinetic match to light particles, relatively easy to purify, and has natural abundance. Its triplet deexcitation lifetime is O(1 us), whereas its singlet deexcitation lifetime is O(10 ns), allowing for excellent pulse shape discrination (PSD) techniques. Xenon emits a longer scintillation wavelength (178 nm vs 128 nm) that is easier to detect for photodetectors. Xenon's fast deecxitation lifetime (O(10

ns)) is good for sharper timing resolution, and xenon has a lower liquid phase ionization energy than argon (9.28 eV vs 14.3 ev).

Xenon-Doped Argon

Xenon-doping of argon is a technique that is currently gaining attention due to its potential to harness advantages of both argon and xenon in a single detector. When xenon is mixed into liquid argon at quantities as low as 10 ppm, the dominant excitation path results in Xe2 dimers that shift the scintillation wavelength to 178 nm, which is more easily detectable and also has a longer Rayleigh scattering length. There is also a poential boost to the ionization yield in the liquid due to the lower ionization energy of xenon, and a possible further increase through a hypothesized Penning process in which xenon is ionized by contact with an excited argon. In dual-phase time projection chambers (TPCs), xenon-doping may improve the electron signal amplification. In this scenario, liquid argon doped with about 2% xenon would provide approximately 50 ppm of xenon in the argon gas due to xenon's lower vapor pressure. At this concentration, drifting electrons in the gas will collide with argon atoms and create ArXe excimers that deexcite at 147 nm. The resulting scintillation wavelength is more efficiently detected than Ar2 light, and the pulse duration would be shorter. Finally, xenon's lower threshold for excitation would ignite more excitations per drifting electron. These benefits from xenon-doping lend themselves to improving projected sensitivities of experiments such as DarkSide-20k and DUNE. Unfortunately, xenon-argon mixtures have a tendancy to form xenon distillation due to the large discrepancies in the phase changes of argon and xenon, making detector homogeniety nontrivial.

As such there are two aspects of xenon-doped argon R&D that necessitate study before implementation into a major experiment. The first is that of stability studies of xenon-doped argon mixtures, which include testing the limits of how much xenon can be doped in the argon before distillation occurs, as well as homogeniety in a heavily-doped mixture on a long term scale. The second is that of quanitfying the aforementioned benefits of doping to detector performance. Both of these studies are being pursued at LLNL with the CHILLAX (CoHerent Ionization Limit in Liquid Argon and Xenon) experiment. In the following section, I will briefly describe the CHILLAX experiment and stability results.

The CHILLAX (CoHerent Ionization Limit in Liquid Argon and Xenon) Experiment

The CHILLAX experiment at LLNL began in 2019 to investigate the challenges and benefits of percent-level xenon-doping in a dual-phase argon TPC. In 2021 a testbed system was developed which was capable of condensing approximately 1 liter of pure liquid argon into a cryostat with pressure stability of +/- 1 mbar. In conventional noble liquid condensation schemes, cold gas is transferred into a cold space where it condenses into liquid and gravity transfers it into the

detector space. If one tried to condense argon gas enriched with 1% xenon (which is below the saturation point of xenon in liquid argon), the xenon gas would freeze at approximately 161 K, around 70 K warmer than the argon gas would begin to condense. To combat this complication, CHILLAX delivers liquid into its cryostat with a two-stage cooling scheme (See Figure 1). First, a heat exchanger vessel with an inner and outer chamber is filled in its inner chamber with liquid argon to the desired liquid height in the main cryostat. Pure argon gas is then delivered to the outer chamber, where it comes in thermal contact with the cold inner chamber and condenses. The liquid argon is pulled by gravity through a delivery line into the base of the detector vessel. After the detector is filled with the desired quantity of liquid argon, circulation to and from the detector vessel to a gas panel begins at approximately 1 L (gas) / minute. The system is then ready for doping. Xenon is introduced into the circulation scheme such that 1% xenon-enriched argon gas makes its way to the outer chamber of the heat exchanger, where it is plunged into liquid argon. In this way, xenon is cooled by a medium that it can dissolve in, and distillation is avoided.

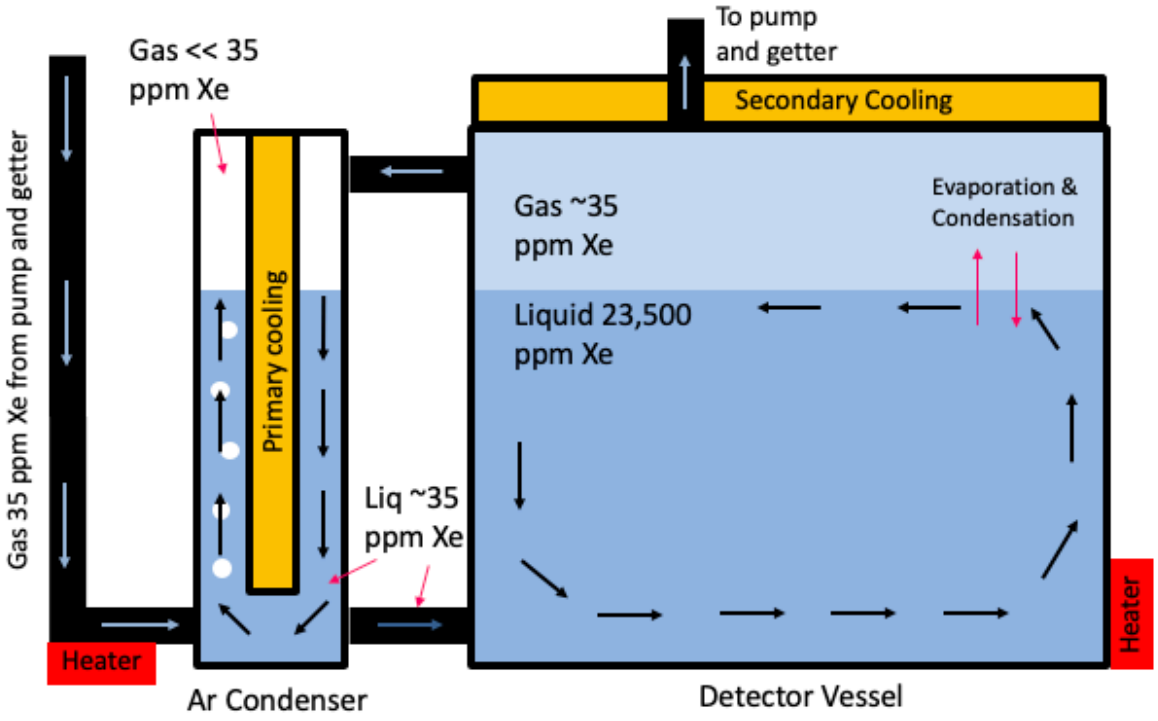

Figure 1: Chillax cooling scheme

In 2022 the focus shifted to stabilizing a percent-level mixture of xenon-doped liquid argon in the CHILLAX cryostat. Numerous instruments were equipped for this effort, including 12 temperature sensors (RTDs), 6 pressure sensors, 2 mass flow controllers (MFCs), a camera mounted on the main cryostat flange that could watch for xenon ice buildup, and a capacitor that could measure xenon concentration in the liquid with 0.05% precision. With careful

manipulation of the system's thermodymamic profile, CHILLAX demonstrated an ability to dope 1 L of liquid argon up to 2.35% xenon (by atomic number) and maintain homogeniety for at least 3 days. Higher doping concentrations and longer time profiles were not conducted due to timing constaints. These stability tests were reported and published in PRC in October 2023 [1].

Progress with the CHILLAX Experiment during HEPCAT Funding

TPC Design and Fabrication Work

After the published stability test (which was known as Run 13), high voltage (HV) feedthrough installation began on CHILLAX. The purpose of these feedthroughs is to supply high voltage to the detector space so a uniform electric field can be made in the TPC. The CHILLAX feedthroughs travel from oil boxes in the air space to the vacuum insulation space through a compression fit seal, and from the vacuum space into the detector space through a metal gasket seal. Due to the extreme difficulty in installing the feedthroughs, once they were tightened in place, their heights are ideally never adjusted again. This highly committal step necessitates careful thought into the height placement of the feedthroughs. To determine the optimal height placement, I designed and fabricated the majority of the TPC that will be used for CHILLAX (See Figure 2). The design was constrained radially by the space between the HV feedthroughs, and the active volume height was chosen to be approximately the diameter as a compromise between maximizing the active volume and avoiding poor light collection efficiency. The TPC model contains a top and bottom array of two 4x4 S13371 SiPM (Silicon Photomultiplier) looking into the volume. Above the bottom array is a grounded shield grid, which protects the array from a ~ -10 kV cathode grid. 1.7" above the cathode is an extraction grid at a slightly lower voltage. Between the grids are electric field shaping rings which increment in voltage steps through 1 GOhm resistors and enclose the active volume. The liquid level is designed to be 5 mm above the extraction grid, and the anode exists 5 mm above the liquid level. The anode hangs from the top SiPM array. After the design phase the grids were fabricated by a company called Great Lakes and the rest of the custom parts were machined by shops partnered with a company called Xometry. Finally, the field shaping rings and grid-holding pieces were mechanically polished by the LLNL metal finishing shop. Prototype SiPM boards were designed in collaboration with LLNL staff physicist Teal Pershing and have been fabricated by Osh Park.

The next step is to surface mount solder the circuit components to the boards and test their performance. After a sufficient board is made, the top SiPM array will be installed with the TPC components into the cryostat. The bottom SiPM array will likely be installed at a later time such that an initial test can be conducted with less complexity. The first iteration of the TPC will then be tested in a cooldown. At this stage, we expect to see our first S1 and S2 light from the TPC, and can characterize their dependence on the xenon concentration.

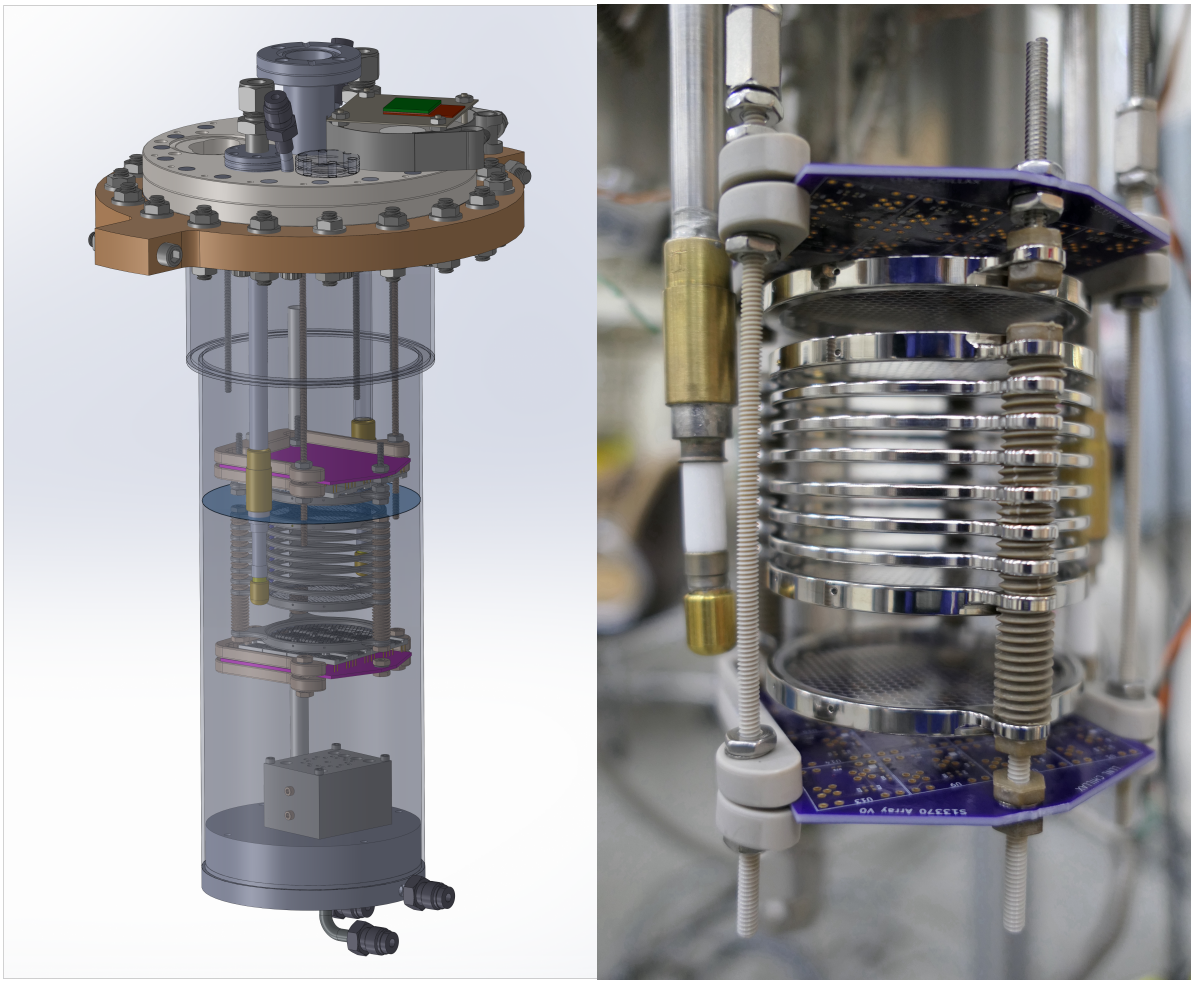

(a) CAD model of CHILLAX cryostat.

(b) Fabrication of TPC Prototype

Figure 2: A resistor chain was installed between the rings after this picture was taken. Notably absent is circuit elements and SiPMs on the SiPM board, which is forthcoming.

CHILLAX Slow Control Work

Before Summer 2023, the power supplies and data acquisition modules for CHILLAX existed as a pile with an undocumented nest of wires connecting them to feedthroughs and the vacuum insulation space. Before the next run, I wanted to organize all of the wiring and modules for CHILLAX such that a handful of DB cables routed out of the detector stand and directly into a breakout box on a 19" rack. The breakout box would route cables into DB cables and wires into its other side which would cleanly plug into the data acquisition box, power supplies, and computers. To start this process, I consolidated external pressure transducers cables on the detector stand into a breakout box, dubbed BB1 (Breakout Box 1). Another set of pressure transducer cables as well as a pair of MFC cables on the gas panel were fed into another breakout box, dubbed BB2 (Breakout Box 2). Each of these breakout boxes had an output DB cable which connected to a much larger breakout box, dubbed BB0 (Breakout Box 0) in a 19" rack, called Deep Blue (See Figure 3). BB0 also received 3 DB cables coming from the vacuum space of CHILLAX. These 5 DB cables carries every pressure and temperature sensor signal, MFC signal, a level meter signal, and transmits +15 V power to all pressure transducers and MFCs. The DB cables also carry power to the 7 heaters (and 2 LEDs) mounted on the system. BB0 contains a 15 V power supply and routes the pressure and temperature signals to a Keithley 6510 DAQ, and routes the MFC signals and level meter directly to the Slow Control Computer, which is named Chillaxsc. BB0 routes the heater and LED power lines to 3 separate power supplies: 1 USB-controlled Keysight 3649A , and 2 ethernet-controlled Rigol DP832As. Deep Blue is equipped with an ethenet switch that manages a local network for CHILLAX, which can access Chillaxsc, a HV crate for SiPM applications, 2 HV crates for TPC applications, the Raspberry Pi, the Rigol power supply, and a Windows computer named Chillindows which continuously acquires capacitance data during detector operation. Finally, Deep Blue is connected to a gateway computer that is accessible remotely through the LLNL VPN. In this way, every instrument and computer in the CHILLAX network can now be remotely monitored and controlled in real time. Finally, detailed documentation of CHILLAX SC wiring and instruments exists on the LLNL Gitlab repository.

CHILLAX Run 14

In December 2023, much of the slow control re-working was completed, along with various upgrades including the completed high voltage. The heat exchanger had also been lifted to accomodate the liquid level height necessary for the future TPC. At this time it was appropriate to conduct a diagnostic run with the system to test many of the upgrades and discover problems that would be evident only during a cooldown. To that end, I condensed approximately 1 liter of pure liquid argon in the cryostat and confirmed that the system could stably operate for over a week. The high voltage feedthroughs were ramped up to -20 kV each and were found to have no issue in pure liquid argon. The three salient issues that were uncovered (and subsequently resolved) in this run were:

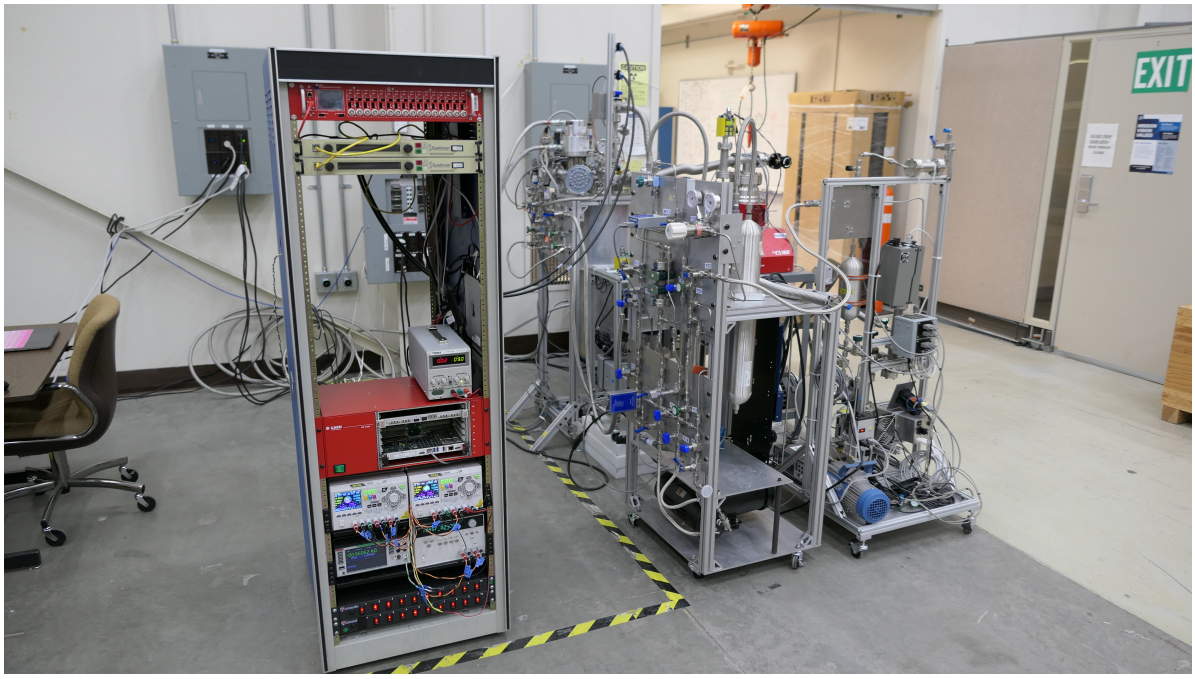

Figure 3: CHILLAX (right) controlled with instruments situated inside of Deep Blue (left)

- **Leaky Upper Thermosyphon:** The thermosyphon volume that cools the detector top flange down was found to leak to a degree such that pressurization of the space up to 1.5 bar resulted in deteriorating the insulating vacuum space from 1e-05 torr to 5e-3 torr. After warming up the detector, we attempted to plug the leak (which was found to exist in a braze joint that connected the copper body to a stainless steel tube) with various solder compounds, but did not have success. We eventually decided to purchase new thermosyphon components with minor geometric modifications and have a professional brazing company do the brazing component of the assembly for us. After completing the part (which included soft soldering two copper bodies together to make the main liquid volume), the part was thermocycled and leak-checked and confirmed to be leak-tight.
- **Heat Leak from Cryostat Bottom:** During detector operation we found that with no heating element being pulsed on the cryostat bottom that there were still O(10) bubbles/second emanating from the base of the cryostat. The likely cause of this was lack of MLI (Multi-Layer Insulation) around the cryostat base. Using the Stefan-Boltzmann radiative law one can compute that for a 4.33" diameter can at 95 K, the radiative heat load on the base of the can from a room temperature (293 K) vacuum insulation can is approximately 3.9 W. To solve this issue for the next run we developed a 15-layer, cup-shaped MLI from mylar (which is PET plastic that is aluminized on one side) and given structural support using brass grommets, clothing tags, and kapton tape. The design was largely guided by LLNL postdoc Samuel Hedges, who developed a similar scheme for a nEXO test stand.

- **Unstable SC Connection and Memory Leak:** The Mac Mini that ran the slow control would lose connection to one of its power supplies within a timescale of a few hours to a couple days. After significant debugging, it was found that the instability was due to a USB-Serial connection between the devices. To counter this issue, a check was placed in the SC where if the connection to the power supply was lost, the connection object would be destroyed and remade. This solved the issue. Another issue that was discovered was a 1 Gb/day memory leak. This was likely caused by increasing the number of controlled power supplies from 1 to 3, increasing the number of controlled MFCs from 1 to 2, and increasing the number of instrument channels for the DAQ to read out. While an effort was made to mitigate the memory leak, the most effective strategy to handle it was upgrading the slow control computer from a Mac Mini with 8 Gb to one with 16 Gb. After these modifications the Slow Control could be run reliably on the scale of one week. Henceforth during operation, the program (and computer) would be restarted every 4-5 days along with the DAQ, which also crashed on a 2-3 week timescale. In this way the system could be reliably operated without unanticipated software crashes.

CHILLAX Run 15

In the beginning of March 2024 we began Run 15 of CHILLAX, which is ongoing at the time of this report submission (March 31st). There are many objectives for this cooldown. These include confirming the resolutions to issues observed in Run 14 are successful during a condensation test, as well as to reconfirm our ability to dope xenon at a degree of concentration and stability that was demonstrated in Run 13. We have also re-installed the capacitor at the base of the cryostat, which is currently monitoring xenon concentration in the cryostat bath (see Figure 4). So far, we have condensed the desired amount of liquid in the cryostat, confirmed that our new MLI mitigates bubbles down to ~1 bubble/minute, and utilized the now leak-tight upper TS to bring the cryostat top flange down to the temperature of the liquid region within 1 K. The slow control is also running smoothly with software restarts every 4-5 days. We have doped the system to 2% xenon in the liquid argon, and plan to continue to match the 2.35% level reached in the stability measurement paper. We will then conduct various stability tests to draw comparisions to past system performance. From there, we will test the the HV feedthroughs in xenon-doped argon, which is expected to perform similarly to the pure liquid argon environment. Next, we will push the doping concentration nearer to the predicted saturation limit. The tentative goal is to stabilize a 5% xenon-argon liquid environment, which at the current operating pressure of 2.125 bar should yield a xenon concentration in the gas of ~90 ppm. At these concentrations, most of the S2 light should be wavelength-shifted to 147 nm Ar-Xe induced deexcitations. HEPCAT fellow Jianyang Qi is currently undertaking work to measure the xenon concentration in the gas using a residual gas analyzer (RGA). The final goal of this run will be to confirm a stable xenon concentration reading in the high O(10 ppm) regime on a scale of multiple weeks. This would demonstrate our ability to reach the desired concentration as well as maintain it for longer timescales, which would be critical to an experiment.

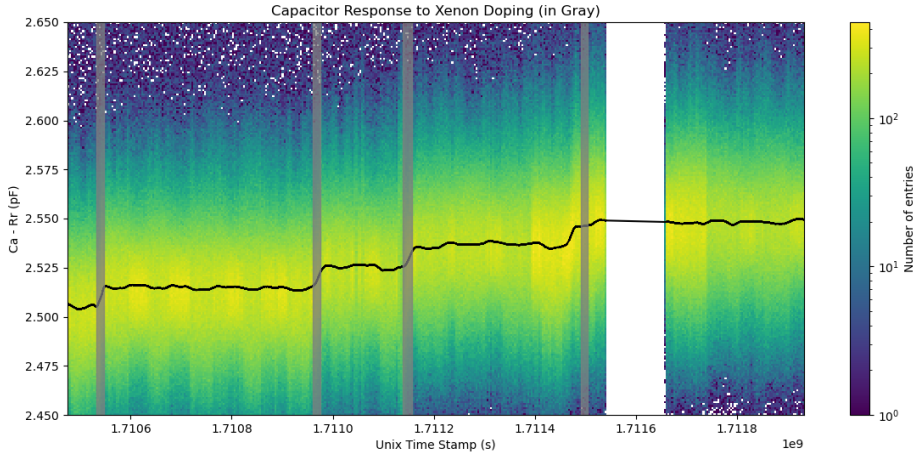

Figure 4: Capacitance data taken during Run 15. Xenon doping regions in gray correspond to doping sessions of 0.5% increments. The time discrepancy between the 4th doping band and the capacitor response is being investigated, but is possibly related to the capacitance meter losing connection for one day shortly after the doping.

Plans for the the remainder of HEPCAT Funding and beyond

Earlier in this report it was mentioned that the two goals of CHILLAX were (loosely put) to investiage the challenges of xenon-doped argon as well as quantify the benefits. After demonstrating the stability of percent-level xenon-doped liquid argon, the experimental focus is transitioning towards preparing for signal improvements to argon from xenon-doping. With this trajectory, we are currently performing engineering runs with CHILLAX to test the numerous upgrades which include the HV feedthroughs, upgraded slow control, and TPC. Once a functioning TPC is installed, there are numerous signal improvement measurements that can be pursued. One such measurement is that of the ionization yield improvement in liquid argon as a function of the xenon concentration. Another example could be to measure the improvement to the S2 in response to doping. Yet another example would be a measurement of the electron extraction efficiency as a function of both the xenon concentration and the extraction field. I anticpate conducting at least one of these measurements during the end of my HEPCAT funding (December 2024) with the goal of publishing the result before the end of my PhD, which ideally would be less than one year later.

References

[1] E. P. Bernard et al. “Thermodynamic stability of xenon-doped liquid argon detectors”. In: *Phys. Rev. C* 108 (4 Oct. 2023), p. 045503. DOI: 10.1103/PhysRevC.108.045503. URL: https://link.aps.org/doi/10.1103/PhysRevC.108.045503.